APPENDIX A: SUPPORTING FIGURES

Figure A1. Relationship of minimum tree diameter versus plot size for the different inventory approaches in the study area. For all inventories, smaller-diameter trees are measured on smaller plots. However, the probability of inclusion of a particular tree size varies among inventories. Legend codes match those used in Tables 1 and 2.

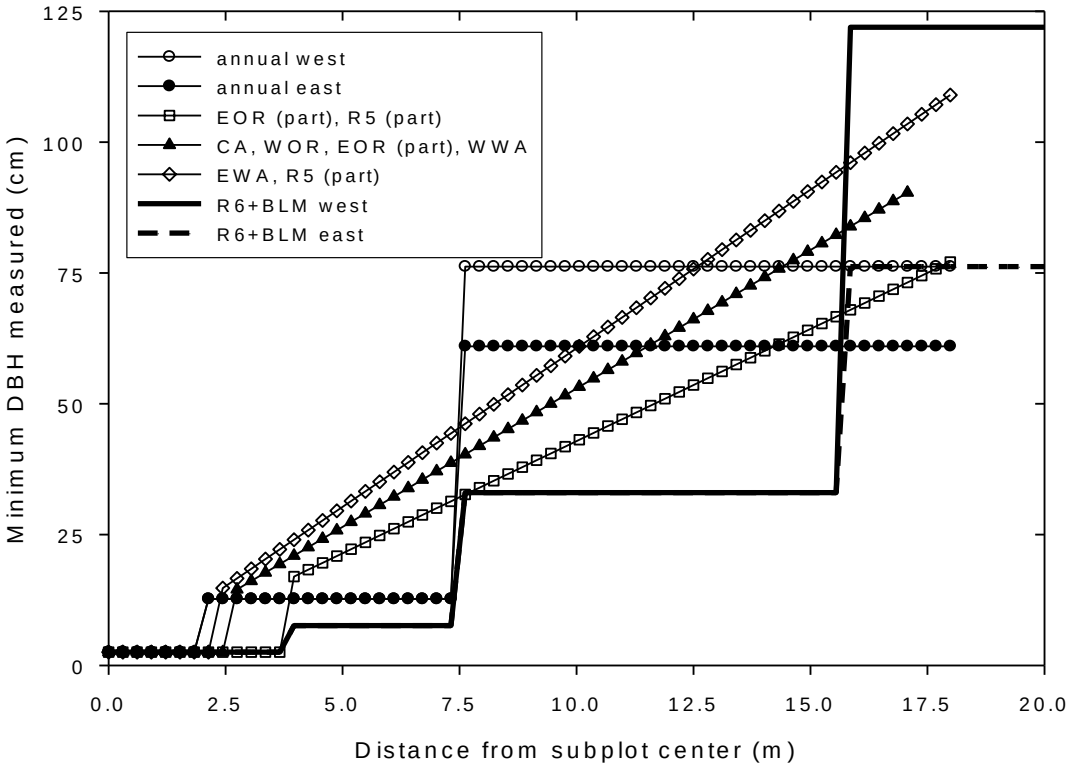

Figure A2. Externally-validated AUC is plotted versus externally-validated $\overline{LogB}$ for comprehensive lists of candidate models generated from NPMR (top and bottom). Values are shown for models generated for three species from the first training sample of the new design, *Arbutus menziesii* (ARME), *Tsuga heterophylla* (TSHE), and *Pinus ponderosa* (PIPO). The numbers of presences varies per species: 301 for *Arbutus menziesii*, 613 for *Tsuga heterophylla,* and 958 for *Pinus ponderosa*. The top axes color code values by species. The color in the bottom axes show the number of predictors or independent variables going into each model.

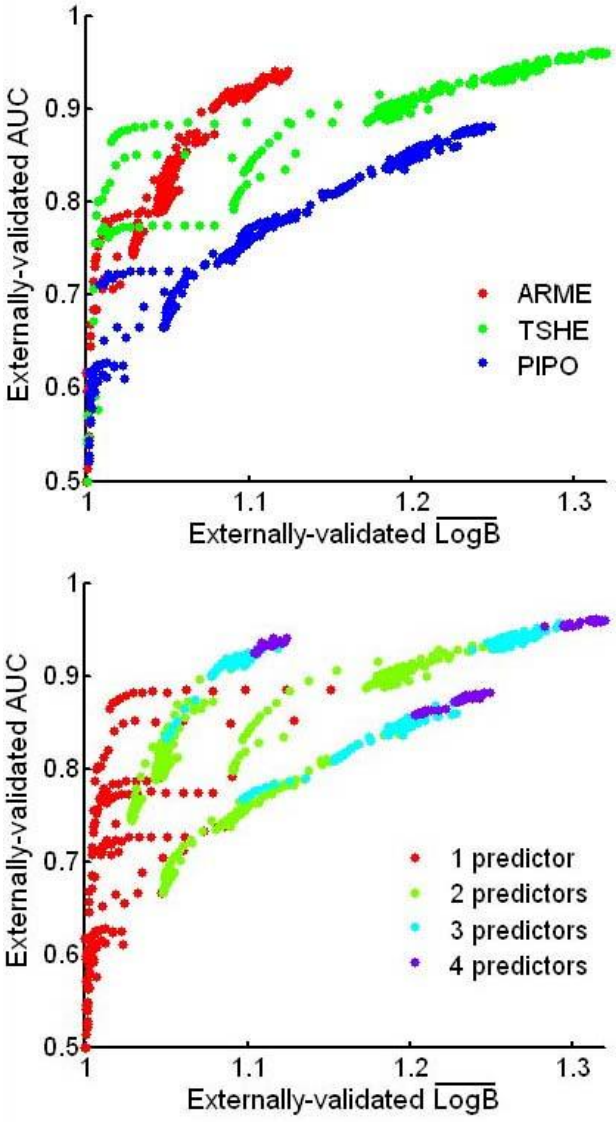

Figure A3. Data were simulated to test the two-sample Kolmogorov-Smirnov statistic (*d*), a measure of effect size, for determination of "climatic bias" among samples of different sizes. 6950 values were generated from normal and bimodal distributions (panel A and B). A pair of random subsamples were taken, one from each distribution, to calculate *d*. This was repeated for 200 replicates across the different sample sizes shown. We plot the means across sample sizes for both comparisons: normal with normal, and bimodal with normal (Figure 5C). The dotted lines represent 95 percent quantiles for the distribution of replicates at each sample size.

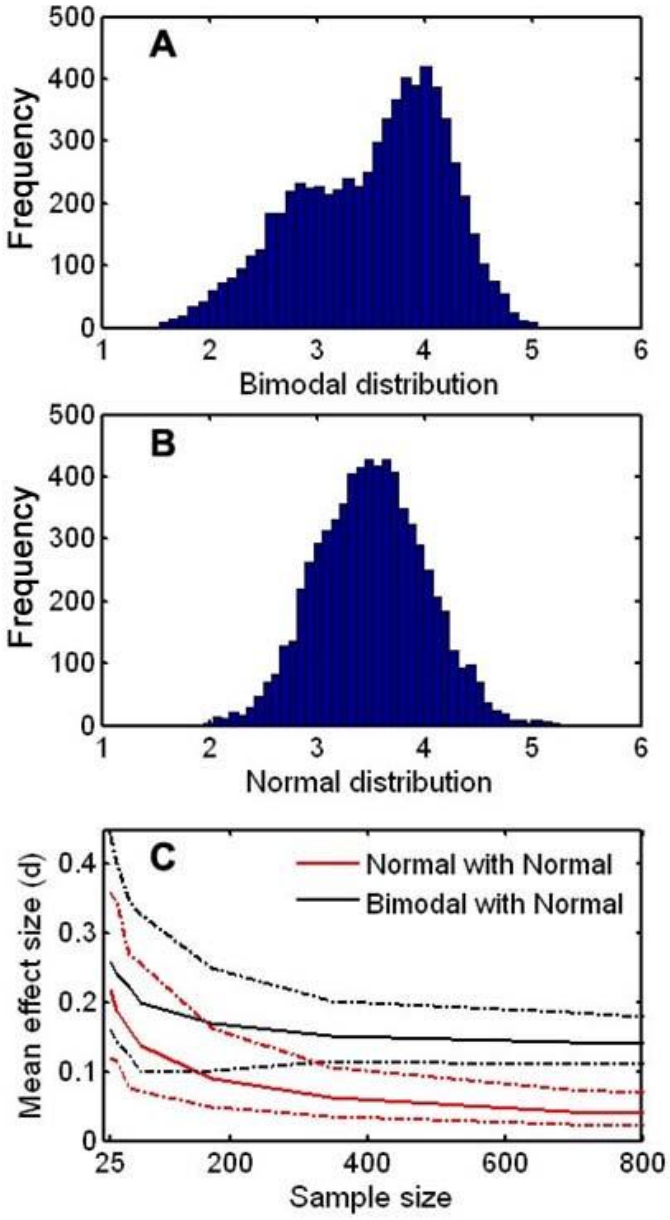

Figure A4. ECDFs (empirical cumulative distribution functions) in the bottom row are generated from simulated distributions shown in the top row at different sample sizes. The figure illustrates the effect of sample size on each ECDF. Small samples yield more jagged ECDFs with a greater likelihood of absolute error among any two compared distributions. The figure also shows how the shape of the ECDF reflects the corresponding shape of the different types of frequency distributions.

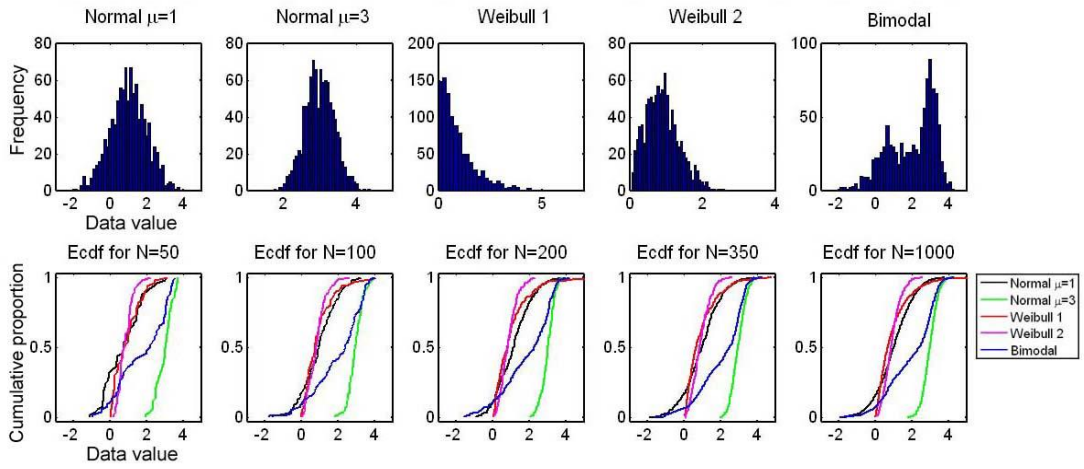

Figure A5. Management regions are shown representing different inventory approaches lumped across the study area for the old inventory. Five distinct geographic regions are demarcated and labeled on the map with boundaries shown by a thin black line (regions correspond to codes for their source name also found in Tables 1 and 2: EWA, WWA, EOR, WOR, and CA). However, two regions are shown by shading (see legend)(R5 and R6+BLMWO).

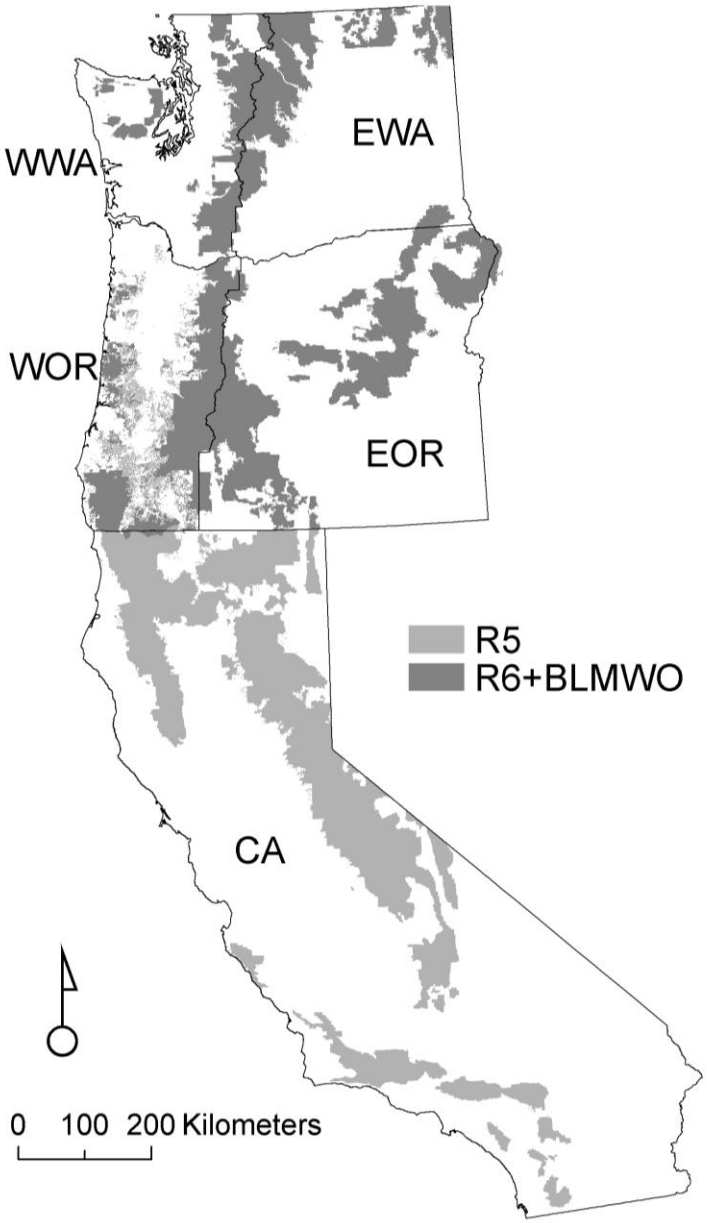

APPENDIX B: SUPPORTING METHODS

Examination of climatic bias with ECDFS and QQ-plots. Our characterization of climatic bias from the data requires explanation. We considered using a measure of effect size, the Kolmogorov-Smirnov Two-Sample Test statistic (*d*) (Massey 1951), to compare climatic bias across different sample sizes (or species with different numbers of presences). This statistic assumes no particular form between the compared distributions, it measures the maximum absolute difference among empirical cumulative distribution functions, and it accommodates differences in both shape and central tendency. However, we checked the immunity of this statistic, *d*, to sample size, and we discovered *d* to depend on sample size using simulated data (see Appendix A; Fig. A3). The shape of the dependence varies with the distributions being tested (Fig. A3). As sampling differences can be reflected not only in the mean but in the shape of a frequency distribution, we instead simply plotted the empirical cumulative distribution functions (ECDFs) from the old and new data sets to visualize the climatic bias per species (Chambers et al. 1983). For each observed value in a distribution, the empirical ECDF plots the fraction of points that are less than the observed value. Numerous ECDFs can be easily condensed and shown in tandem, and they represent the mean, standard deviation, and standardized third and fourth moments all in one figure (Wilk and Gnanadesikan 1968). We also used quantile-quantile plots (QQ-plots) of two distributions to graphically investigate evidence for climatic bias with four species. QQ-plots show empirical quantiles from two samples plotted against each other to determine if they come from the same distribution (Chambers et al. 1983). QQ-plots are a powerful approach to zoom in and compare shape of distributions underlying two samples of data. However, confidence bounds on QQ-plots that compare two unknown distributions are not possible due to issues regarding multiple comparisons and resulting uncertainty (Chambers et al. 1983).

While other statistical tests exist, many are based on comparisons among histograms. The biggest problem we see with using histograms is that the binning is arbitrary. Results will differ depending on bin size and how the partitions fall relative to structure in the data. ECDFs don't require binning. Further, the ECDFs and QQ-plots provided here show the data and comparisons of interest for anyone concerned.

Chambers, J.M., Cleveland, W.S., Kleiner, B., and Tukey, P.A., 1983. Graphical Methods for Data Analysis. Wadsworth Publishing Company, Belmont, CA.

Massey, F.J. Jr., 1951. The Kolmogorov-Smirnov test of goodness of fit. Journal of the American Statistical Association, 46, 68-78.

Wilk, M.B., Gnanadesikan, R., 1968. Probability plotting methods for the analysis of data. Biometrika Trust, 55, 1-17.